energies

Article

Vacuum Insulation Panel: Evaluation of Declared Thermal Conductivity Value and Implications for Building Energy

Fred Edmond Boafo [1], Jin-Hee Kim [1], Jong-Gwon Ahn [1], Sang-Myung Kim [2] and Jun-Tae Kim [3,*]

[1] Green Energy Technology Research Center, Kongju National University, Cheonan 31080, Republic of Korea
[2] Zero Energy Buildings Laboratory, Graduate School of Energy Systems Engineering, Kongju National University, Cheonan 31080, Republic of Korea
[3] Department of Green Smart Architectural Engineering, Kongju National University, Cheonan 31080, Republic of Korea
* Correspondence: jtkim@kongju.ac.kr; Tel.: +82-41-521-9333

Abstract: Policymakers regularly implement stricter building energy-efficiency codes towards curtailing building energy use. Inevitably, super-insulating materials such as Vacuum Insulation Panels (VIPs) are essential to satisfy such codes. VIPs have been applied to buildings for over two decades now, with many lessons learned. Generally, the thermal conductivity values of VIPs often reported in the literature are the center-of-panel thermal conductivity (λ_{cop}) and effective thermal conductivity (λ_{eff}), factoring thermal bridges. However, there are other indexes, such as $\lambda_{90/90}$ (declared value in the 90% percentile with a confidence of 90%) and $\lambda_{\text{cop,90/90,aged}}$ (factoring aging), that increase consistently and reliably in the declared thermal conductivity value for VIPs. These indexes are scarcely computed and hardly reported. The main aim of this study was to examine the different declared thermal conductivity values of VIP-based guidelines, such as draft ISO DIS 16478, and evaluate their implications on annual building energy consumption. The main study constitutes four parts: (1) experimental evaluation of the thermal properties of pristine and aged VIP samples, (2) computation of thermal conductivity indexes, (3) numerical investigation of thermal conductivity indexes based on a reference building, and (4) related building energy implications. The mean λ_{cop} for 10 VIP samples was 0.0042 W/(mK) and increased to 0.0073 W/(mK) for $\lambda_{90/90}$, bridge, aged. Results show a significant bearing on building energy performance of as much as 2.1 GJ.

Keywords: vacuum insulation panel (VIP); thermal conductivity; building energy; experimental evaluation; numerical modeling

check for updates

Citation: Boafo, F.E.; Kim, J.-H.; Ahn, J.-G.; Kim, S.-M.; Kim, J.-T. Vacuum Insulation Panel: Evaluation of Declared Thermal Conductivity Value and Implications for Building Energy. *Energies* **2023**, *16*, 5841. https://doi.org/10.3390/en16155841

Academic Editor: Luisa F. Cabeza

Received: 8 July 2023
Revised: 2 August 2023
Accepted: 3 August 2023
Published: 7 August 2023

1. Introduction

Energy generation and utilization across various sectors of the economy are responsible for significant greenhouse gas emissions. Energy efficiency is currently the focus of numerous stakeholders. With the recent emergence of Passive Houses, Zero-Energy Buildings, and the Green House Project, there have been concerted efforts to enable buildings to manage their energy usage independently while minimizing energy consumption. Stakeholders tackling energy-efficient façades and building systems are conversant with the household name, Vacuum Insulation Panel (VIP). Steadily gaining ground in the building industry for decades now [1–4], VIP is a material system composed of a porous core matrix, evacuated, and wrapped in a gas/vapor-tight laminate envelope that is heat-sealed at the edge or surface of the panel. For example, considering an upper limit center-of-panel thermal conductivity (λ_{cop}) of 0.004 W/(mK) for a pristine VIP with fumed silica core material and a typical value of 0.008 after 25 years, VIP has about 5–10 times better thermal performance compared to other traditional insulation materials of today [5]. For such low thermal conductivity, albeit measured at the center-of-panel, thermal bridges become more pronounced; especially in building applications where other materials with varied thermal properties are sandwiched with VIPs. Generally, thermal bridges for constructions with

VIP (also called Vacuum Insulated Sandwich Elements (VISE)) can be categorized into three levels [6]. Firstly, thermal bridges are at the individual VIP system level and are attributed to differences in thermal properties between the core material and laminate envelope of VIPs. Secondly, thermal bridges at the VIP level are due to air gaps between adjacent VIPs and mounting spacers or disparities in thermal conductance between VIPs and joint materials. The final category of thermal bridges for VISE is at building façade level. This is because of differences in thermal characteristics between VIPs and other building envelope components. Some studies have scrutinized thermal bridges for individual VIP [7] or VISE, based on either numerical or experimental methods, or both [8]. Particularly, it was reported that the influence of the edge effect cannot be neglected for a realistic declaration of the effective thermal conductivity (λ_{eff}) of VIPs [9]. Together with thermal bridges, the effect of VIP aging with time on the resultant thermal conductivity cannot be marginalized. Earlier studies established that the change in VIP thermal conductivity with aging is due to a gas pressure increase in the panel and moisture accumulation and can be expressed by Equation (1) [10]:

$$\frac{\partial\lambda}{\partial t} = \frac{\partial\lambda}{\partial p}\frac{\partial p}{\partial t}(T,\varphi) + \frac{\partial\lambda}{\partial X_W}\frac{\partial X_w}{\partial t}(T,\varphi) \tag{1}$$

where $\partial\lambda/\partial t$ is the change in thermal conductivity with time [10^{-3} (W/(mKyr)], $\partial\lambda/\partial p$ is the change in thermal conductivity due to pressure [W/(mKbar)], $\partial p/\partial t$ is the pressure increase rate (mbar/yr), $\partial\lambda/\partial X_W$ is the change in thermal conductivity due to humidity [10^{-3} W/(mKM-%)], $\partial X_W/\partial t$ is the moisture accumulation rate (%-mass/yr), T is the temperature (K), and φ is the humidity (%). Under the framework of the International Energy Agency's ECBCS Annex 39, Equation (1) was defined in similar terms by Equation (2) [11]:

$$\lambda_a(t) = \lambda_{90/90} + \lambda_p \cdot p_a \cdot t + \lambda_{XW} \cdot X_{W,eq} \cdot \left(1 - e^{(-t/\tau)}\right) \tag{2}$$

where $\lambda_{90/90}$ is 90% fractile with a confidence level of 90% for the thermal conductivity (W/mK), λ_p is the pressure dependent increase of the thermal conductivity (W/mK.Pa.yr), p_a is the annual increase of internal pressure of the VIP (Pa/yr), t is a time constant (yr), λ_{XW} is the humidity dependent increase of the thermal conductivity (W/mK)/mass-%, $X_{W,eq}$ is the water content at 23 °C, 50% RH (mass-%), and τ is the time constant humidity compensation mass-%/(mass-%/yr). Specifically, for VIPs with fumed silica core material, an additional aging factor has been reported to be due to long-term changes in the fumed silica skeleton induced by the migration of physisorbed H_2O molecules and dissolved ions containing Si and O [12]. Based on the previous studies, a more recent study briefly summarized the factors contributing to the long-term thermal conductivity of VIPs as follows: (i) gas permeation through VIP laminate envelope barriers, (ii) water vapor diffusion into the core material of VIPs, (iii) aging of VIPs' own core material, and (iv) aging of VIPs' own envelope. Nonetheless, in the open literature, the thermal conductivity value often reported for VIPs is the thermal conductivity measured at the center of the panel without thermal bridges (λ_{cop}) or λ_{eff}, including thermal bridges along the edge of the panel only. Other thermal conductivity indexes described in draft ISO 16478 [13], such as $\lambda_{90/90}$, which is declared thermal conductivity in the 90% percentile with reliability of 90% (also referred to in Equation (2)), and $\lambda_{90/90\ ,aged}$ ($\lambda_{90/90}$ plus aging effect), are commonly not reported. This is because more samples are required (minimum of 10 samples for each VIP size). Also, it takes a long time for such declarations, especially when factoring in the aging effect. Typically, accelerated aging tests under extreme conditions must be carried out for not less than 6 months to determine the degradation of VIPs and the aging effect on their thermal properties. Not to mention the perceived difficulties concerning procedures, the data required, and the calculation methods involved. Apart from studies by Brunner et al. [14], the authors found no other works in the literature that purposefully computed values for $\lambda_{90/90}$.

Regarding the numerical characterization of VIP either on a component scale or a whole building scale, various researchers have employed slightly different modeling approaches. As summarized in Table 1, the first of two common approaches involves using VIPs' effective thermal conductivity value, which is the thermal conductivity measured at the center of the panel plus an added term for linear thermal transmittance. The second method simplifies VIPs' actual multilayer envelope structure into a single homogenous layer. The combined effects of thermal bridges, aging, and particularly the 90% percentile with a reliability of 90% remain to be considered in such studies.

Table 1. Review of previous works on VIP modeling schemes.

Reference	Method	Description of VIP Modeling Technique
Lorenzati et al. [15]	Numerical simulations using Physibel BISCO software	VIP envelope was simplified into a simple, equivalent, homogenous layer
Ghazi Wakili et al. [9]	Numerical simulations using Physibel TRISCO software	VIP envelope was simplified into a simple, equivalent, homogenous layer
Boafo et al. [16,17]	Numerical simulations using Physibel BISCO software	VIP component was modeled with the effective thermal conductivity value
Batard et al. [18]	Numerical simulations using Physibel Dymola software	VIP component was modeled with the effective thermal conductivity value
Park et al. [19]	Numerical simulations using Physibel TRISCO software	VIP component was modeled with the effective thermal conductivity value
Kim et al. [20]	Numerical simulations using Physibel BISCO software	VIP component was modeled with the effective thermal conductivity value

In this regard, the main purpose of this study was to examine a range of thermal conductivity indexes for VIPs, based on draft ISO 16478. From an energy modeling perspective, the difference in energy consumption by implementing one thermal conductivity index over the other for a building model is investigated as well. It is worth mentioning that the term 'thermal conductivity indexes' is solely introduced in this study to encompass the various possible thermal conductivity values for VIPs, considering or not considering factors such as thermal bridges, aging, and the 90% percentile with a reliability of 90%. As far as the authors know, this paper is the first to cover various thermal conductivity indexes of VIPs and related building energy use.

2. Methods

This section reports details of the experimental and numerical methods used in this study. The section commences by introducing and clearly defining eight thermal conductivity indexes for VIPs. Then, in-lab experimental procedures employed to evaluate the thermal properties of VIPs for computing thermal conductivity indexes are reported. Afterwards, detailed descriptions and modeling operations are reported for a real reference building with VIPs installed that is used as a baseline to verify the impact of the various thermal conductivity indexes on the computed annual energy demand.

2.1. Definition of Thermal Conductivity Indexes for VIPs

The term 'thermal conductivity indexes' is introduced and solely used in this study to include the levels of thermal conductivity values of VIPs, including a factor for thermal bridge only, aging effect only, 90% percentile values with 90% reliability only, or a combination of the three factors. The baseline thermal conductivity index is the mean center-of-panel thermal conductivity (λ_{cop}) measured at the center of the panel, without accounting for other factors. The second thermal conductivity index is thermal conductivity based on 90% percentile values with 90% reliability ($\lambda_{90/90}$). This is the declared thermal conductivity in the 90% percentile with a reliability of 90% based on λ_{cop}, and not accounting for other factors as well. To be in line with standards EN 13162 to EN 13167 of conventional insulation [21–26], $\lambda_{90/90}$ introduces a factor of reliability or tolerance that considers production deviation [14]. $\lambda_{90/90}$ can be calculated based on Equation (3):

$$\lambda_{cop,90/90} = \lambda_{mean} + k.s_{\lambda} \tag{3}$$

and s_{λ} is given by:

$$s_{\lambda} = \sqrt{\frac{\sum_{i-1}^{n}(\lambda_i - \lambda_{mean})^2}{n-1}} \tag{4}$$

where λ_i is one test result of thermal conductivity, n is the number of test results/samples, λ_{mean} is the mean thermal conductivity of n samples, and k is a factor related to the number of test results/samples. For instance, for the 10 test samples used in this study, the value of k is 2.07. Thirdly, the mean center-of-panel thermal conductivity plus thermal bridge ($\lambda_{cop,bridge}$) is the thermal conductivity index measured at the center of the panel, plus an additional term for the thermal bridge effect along the edge of the panel. The edge effect (Δ_{edge}) and $\lambda_{cop,bridge}$ can be computed using Equations (5) and (6), respectively [9]:

$$\Delta_{edge} = \psi(d) \times d \times p/A \tag{5}$$

$$\lambda_{cop,bridge} = \lambda_{cop} + \Delta_{edge} \tag{6}$$

where $\psi(d)$ is the linear thermal transmittance at the edge of the panel (W/(mK)) and d, p and A are the thickness (m), perimeter (m), and area (m^2) of the panel, correspondingly. It is worth noting that this specific thermal conductivity index, $\lambda_{cop,bridge}$, is often referred to as the effective thermal conductivity of VIPs in the literature. The next thermal conductivity index is thermal conductivity based on 90% percentile values with 90% reliability, plus the effects of the thermal bridge ($\lambda_{90/90,\mathrm{bridge}}$). Whereas the thermal conductivity indexes mentioned in the preceding paragraphs are based on pristine VIPs, the next indexes are based on aged VIPs to account for the VIP aging effect. The basic index is thermal conductivity measured at the center of aged VIPs ($\lambda_{cop,\mathrm{aged}}$). On top of that, ($\lambda_{90/90,\mathrm{aged}}$) represents thermal conductivity in the 90% percentile with a reliability of 90% calculated for aged VIP samples using Equation (1) and based on ($\lambda_{cop,\mathrm{aged}}$) values. The seventh index is the mean thermal conductivity measured at the center of aged VIPs plus thermal bridge effects ($\lambda_{cop,\ bridge,\ age}$). Finally, ($\lambda_{\ 90/90,\mathrm{bridge,aged}}$) includes thermal bridge and aging factors for thermal conductivity values based on 90% percentile values with 90% reliability. A summarized description of the thermal conductivity indexes, showing factors accounted for in each index, is summarized in Table 2.

Table 2. Brief description of thermal conductivity indexes for VIPs.

Case #	Description of Thermal Conductivity Indexes	Thermal Bridge	90%/90% Reliability	Aging Effect
1	Mean center-of-panel thermal conductivity (λ_{cop}), W/(mK)	No	No	No
2	Thermal conductivity based on 90% percentile values with 90% reliability ($\lambda_{90/90}$), W/(mK)	No	Yes	No
3	Mean center-of-panel thermal conductivity, plus thermal bridge ($\lambda_{cop,bridge}$), W/(mK)	Yes	No	No
4	Thermal conductivity based on 90% percentile values with 90% reliability, plus thermal bridge ($\lambda_{90/90,\ \mathrm{bridge}}$), W/(mK)	Yes	Yes	No

Table 2. *Cont.*

Case #	Description of Thermal Conductivity Indexes	Thermal Bridge	90%/90% Reliability	Aging Effect
5	Mean center-of-panel thermal conductivity, plus aging ($\lambda_{cop,\text{aged}}$), W/(mK)	No	No	Yes
6	Thermal conductivity based on 90% percentile values with 90% reliability, plus aging ($\lambda_{90/90,\text{aged}}$), W/(mK)	No	Yes	Yes
7	Mean center-of-panel thermal conductivity, plus aging and thermal bridge effects ($\lambda_{cop,\text{bridge,aged}}$), W/(mK)	Yes	No	Yes
8	Thermal conductivity based on 90% percentile values with 90% reliability, plus thermal bridge, and aging effects ($\lambda_{90/90,\text{bridge,aged}}$), W/(mK)	Yes	Yes	Yes

2.2. Experimental Assessment of VIP Properties and Aging Procedures

All materials, including VIP samples investigated in this study, are commercial grade. The VIPs were composed of fumed silica core material encapsulated in a metalized laminate envelope, with dimensions of 300 mm × 300 mm × 20 mm. In all, 10 VIP samples were tested and used in this study. The center-of-panel thermal conductivity of each VIP was examined using heat flow thermal conductivity instrumentation (Netzsch HFM 436). The working principle of a heat flow meter is based on Fourier's law of thermal conduction, represented mathematically by Equation (7) [27]:

$$Q = \lambda_T A\ (\Delta T/d) \tag{7}$$

where Q is the heat flow (W), λ_T is the thermal conductivity of a sample (W/(mK)), ΔT is the temperature gradient (K) through an area A (m^2), and d is the thickness of a sample (m). A generalized schematic diagram illustrating the components and working principle of a heat flow meter is shown in Figure 1.

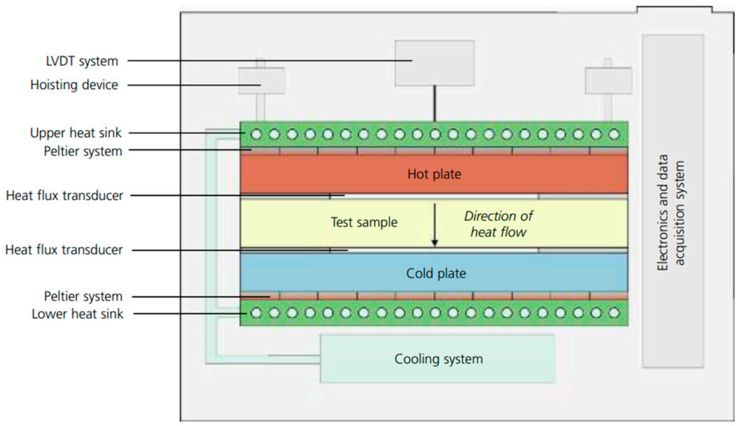

Figure 1. Schematic showing heat flow meter instrumentation [28].

The test specimen is placed between the hot and cold plates, which are controlled to a defined mean sample temperature and temperature drop to measure the heat flowing through the specimen. The heat flow through the specimen is then measured by calibrated heat flux transducers over a metering area of the test specimen. After reaching equilibrium, the test is performed, and the specimen's thermal conductivity value is computed automatically by the test instrumentation's electronic system. During thermal conductivity tests, the hot and cold plate temperatures used were 15 °C and 5 °C, respectively;. at both mean temperature (Tm) and change-in-temperature (ΔT) of 10 °C. To evaluate linear thermal transmittance (thermal bridge) along the edge of the panel, 2 VIPs were placed adjacent to each other at their seams and tested in a larger heat flow meter test apparatus (EKO

HC-074) that accommodated the specimen sizes. Accelerated aging for VIPs was carried out in a climatic chamber (Jeio Tech TH-G-1000) for 180 days at a temperature of 70 °C and a relative humidity of 50%. Actual images of one VIP sample and the test equipment are shown in Figure 2, while relevant details and measurement accuracies specified by the manufacturers are summarized in Table 3.

(**a**)

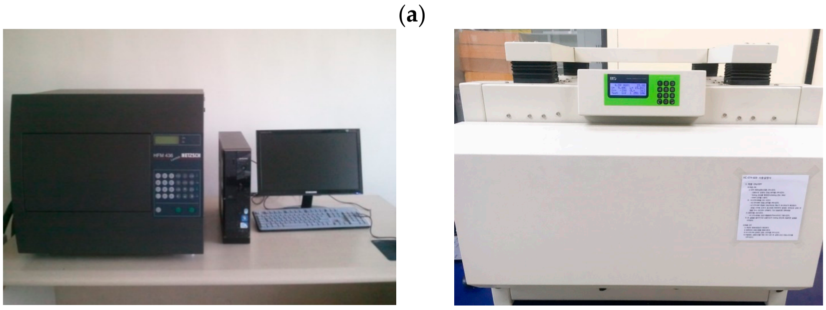

(**b**)

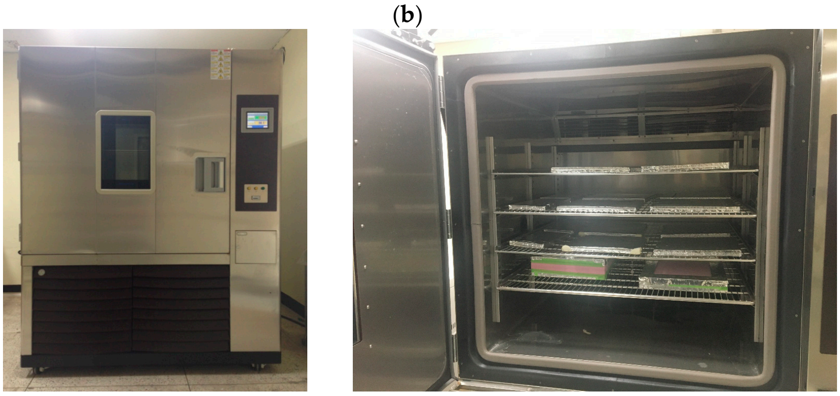

(**c**)

Figure 2. Picture of test apparatus: (**a**) VIP sample, (**b**) heat flow meter (Netzsch 436—**top left**; EKO HC-074—**top right**), and (**c**) temperature-humidity climatic chamber (external view—**bottom left**; internal chamber—**bottom right**).

Table 3. Details and measurement accuracies of test apparatus.

Equipment Type (Model)	Specifications
Heat flow meter to estimate center-of-panel thermal conductivity (Netzsch 436)	Temperature range: −30 °C to +90 °C Accuracy: ±1% to 3% Repeatability: 0.5% Maximum specimen size: 0.3 m × 0.3 m × 0.1 m
Heat flow meter for thermal bridge evaluation (EKO HC-074)	Temperature range: −15 °C to +80 °C Accuracy: >1% Repeatability: 0.2% Maximum specimen size: 0.6 m × 0.6 m × 0.2 m
Temperature and humidity climatic chamber for accelerated aging (JEIO TECH TH-G-1000)	Temperature range: 15 °C to 90 °C Temperature fluctuation: ±0.3 °C at 40 °C/75% RH Humidity range: 25% RH to 95% RH Humidity fluctuation: ±1% RH at 75% RH/40 °C

2.3. Reference Building Description

The reference building is an existing south-facing two-story (above-ground) residential building. The building has been insulated with 20 mm VIPs on the external walls and was one of the case studies considered as part of the International Energy Agency's Energy in Buildings and Communities Programme under Annex 65 (Long-term performance of super-insulating materials in building components and systems) [29]. The total conditioned floor area of the building is about 171 m^2, with a floor height of 3.6 m, and it is located in Seongnam City, Republic of Korea. Figure 3a depicts the real pictures of the reference building, while a rendered 3D image displaying the sun's path on a representative hot summer day (i.e., 6 August) at 15:00, direct solar radiation on the roof, and cast shadows of the building façade and adjacent buildings are shown in Figure 3b. Similarly, the respective thermal zones for the first and second floors are depicted in Figure 4. The components for the external wall and roof and relevant thermophysical properties are summarized in Table 4. The nominal *U*-values for the external wall and roof of the reference building are 0.12 W/(m^2K) and 0.16 W/(m^2K), correspondingly.

(**a**)

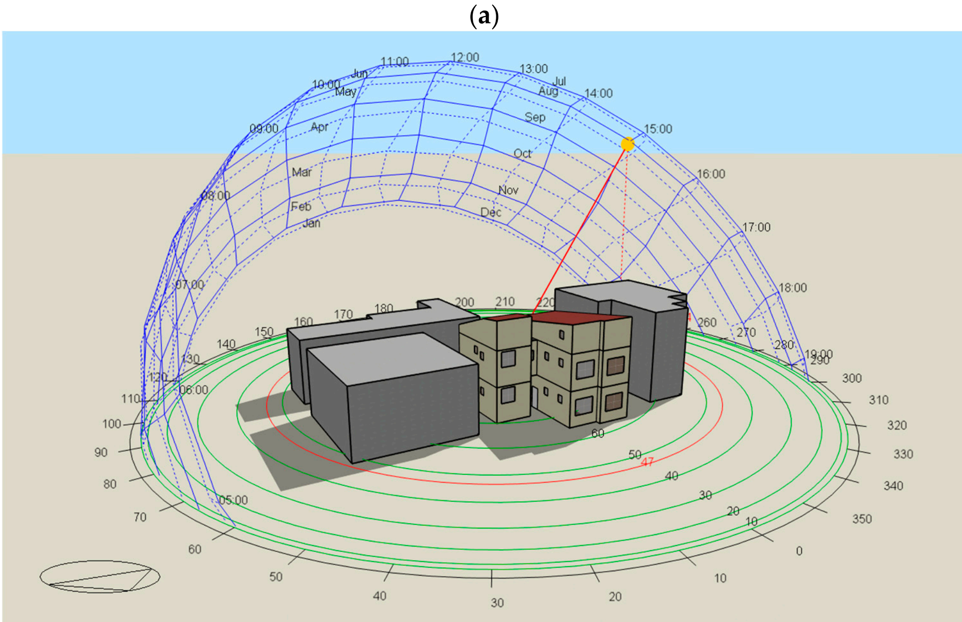

(**b**)

Figure 3. Reference building: (**a**) real pictures and (**b**) a rendered 3D image showing the sun's path and cast shadows.

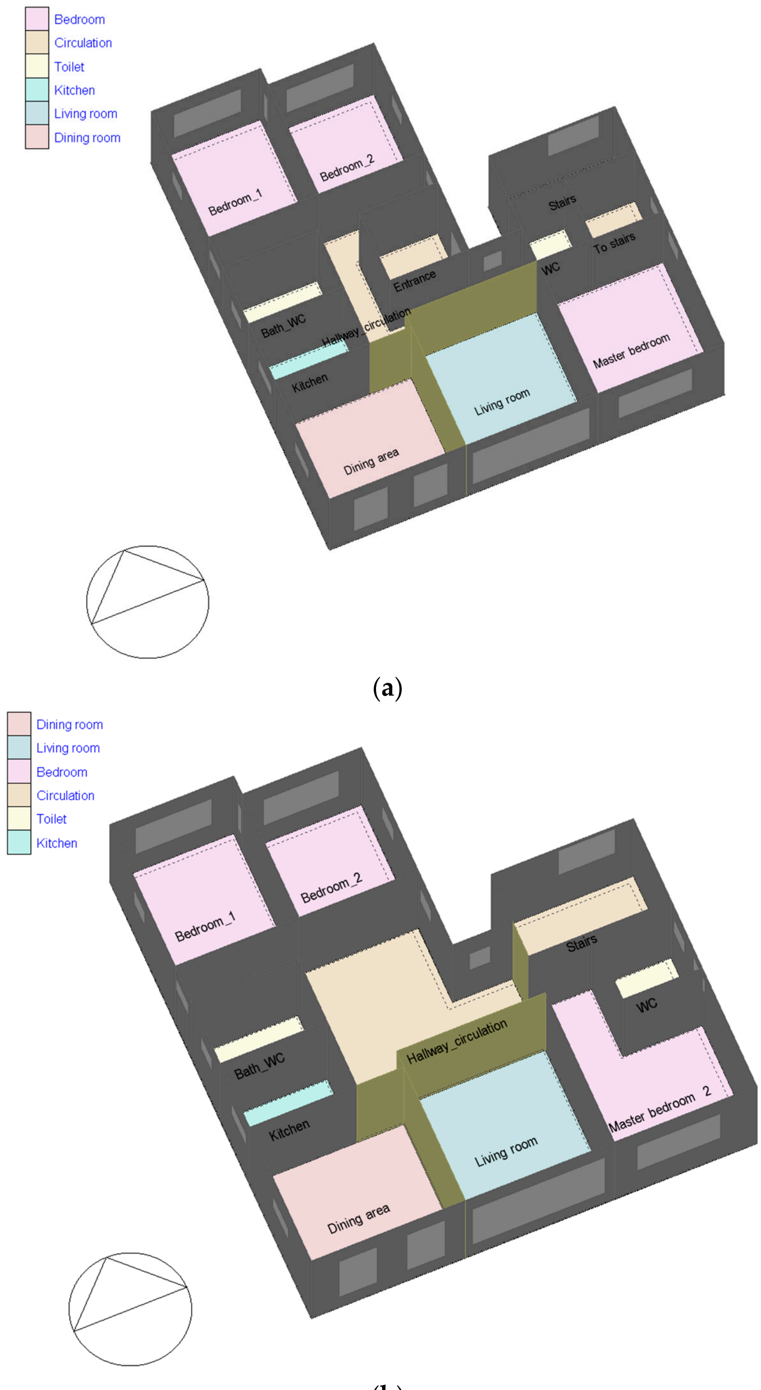

Figure 4. Floor plan layout showing various thermal zones. (**a**) First floor unit; (**b**) Second floor unit.

Table 4. Reference building—component layers and thermophysical properties.

Layer	Material	Thickness (m)	Thermal Conductivity W/(mK)	Density kg/m^3	Specific Heat J/(kgK)
		Reference wall			
Innermost layer	OSB	0.011	0.13	650	1700
Layer 2	VIP	0.02	0.0042	800	200
Layer 3	Cellulose insulation	0.08	0.04	48	1381

Table 4. *Cont.*

Layer	Material	Thickness (m)	Thermal Conductivity W/(mK)	Density kg/m^3	Specific Heat J/(kgK)
Layer 4	OSB	0.011	0.13	650	1700
Layer 5	Air gap *	0.010	-	-	-
Layer 6	EPS	0.035	0.04	15	1400
Layer 7	OSB	0.011	0.13	650	1700
Outermost layer	Wood finishing	0.011	0.12	510	1380
		Reference roof			
Innermost layer	Gypsum plastering	0.019	0.40	1000	1000
Layer 2	Cellulose insulation	0.235	0.04	48	1381
Layer 3	Waterproof	0.005	0.17	1050	1000
Layer 4	OSB	0.011	0.13	650	1700
Layer 5	Roofing felt	0.015	0.19	960	1000
Outermost layer	Asphalt shingles	0.01	0.70	2100	1000

* Thermal resistance of air gap = 0.15 (m^{2}W/K).

The window type is double LoE glazing (Clear 3 mm/13 mm Argon) with a solar heat gain coefficient (SHGC) of 0.69, a light transmittance (LT) of 0.74, and an overall U-value of 1.72 (based on ISO 10292 specifications [30]). All external surfaces of the building are exposed to external environmental conditions.

2.4. Building Modeling, Operations, and Schedules

The reference building was modeled with DesignBuilder software. DesignBuilder is a commercially available and tested high-end building environmental design software capable of performing complex building modeling analysis including energy and comfort, HVAC, daylighting, cost, design optimization, CFD, BREEAM/LEED credits, and reports complying with several national building regulations and certification standards [31]. The computations in DesignBuilder are based on the EnergyPlus v9.4 engine. Structural data for the reference building were used as inputs for the building modeling. Also, numerical inputs for VIPs were based on experimental data. Although the building uses an EHP system for space conditioning, for the purpose of this study, an Ideal Load Air System (ILAS) heating, ventilation, and air conditioning (HVAC) system was modeled to evaluate space heating and cooling loads. ILAS is an ideal unit that simply adds or removes heat and moisture from a zone by mixing air at the zone exhaust condition with outdoor air based on specified conditions [32]. Since the purpose of this study is to examine the impact of various thermal conductivity indexes on VIPs, using the same HVAC system for all the cases implies that the outcomes are reliable and not determined by the type of HVAC system modeled. The HVAC relied on thermostat set points, which were set to 21 °C and 24 °C for heating and cooling, respectively. Additionally, according to the dominant space conditioning requirement, heating and cooling seasons were scheduled from November to April and May to September, respectively. For annual simulations, weather data from Seongnam (World Meteorological Station No. 471110 and derived between 2007 and 2021) in EPW format was used. Table 5 summarizes the occupancy density, electric plug load intensity, and lighting demand intensity for the various thermal zones.

Table 5. Standard inputs for modeling operations.

Zone	Occupancy Density People/100 m^2	Electric Plug Load Intensity W/m^2	Light Density W/m^2
Bedroom	0.0229	3.58	15
Living room	0.0188	3.90	15
Kitchen	0.0237	30.28	15
Dining area	0.0169	3.06	15
Bath/WC	0.0243	1.61	15
Stairs	0.0155	1.57	15
Hallway/circulation	0.0155	1.57	15

3. Results

In this section, key findings from experimental assessments and numerical computations are discussed.

3.1. Thermal Characterization of VIPs

Table 6 shows the results and range for the eight thermal conductivity indexes for VIPs.

Table 6. Thermal conductivity indexes for VIPs (size: 300 mm × 300 mm × 20 mm).

Case #	Description of Thermal Conductivity Indexes	Data
1	Mean center-of-panel thermal conductivity (λ_{cop}), W/(mK)	0.00417
2	Thermal conductivity based on 90% percentile values with 90% reliability ($\lambda_{90/90}$), W/(mK)	0.00427
3	Mean center-of-panel thermal conductivity, plus thermal bridge ($\lambda_{cop,\mathrm{bridge}}$), W/(mK)	0.00630
4	Thermal conductivity based on 90% percentile values with 90% reliability, plus thermal bridge ($\lambda_{90/90,\mathrm{bridge}}$), W/(mK)	0.00641
5	Mean center-of-panel thermal conductivity, plus aging ($\lambda_{cop,\ \mathrm{aged}}$), W/(mK)	0.00499
6	Thermal conductivity based on 90% percentile values with 90% reliability, plus aging ($\lambda_{90/90,\mathrm{aged}}$), W/(mK)	0.00515
7	Mean center-of-panel thermal conductivity, plus aging and thermal bridge effects ($\lambda_{cop,\mathrm{bridge,aged}}$), W/(mK)	0.00713
8	Thermal conductivity based on 90% percentile values with 90% reliability, plus thermal bridge and aging effects ($\lambda_{90/90,\mathrm{bridge,aged}}$), W/(mK)	0.00728

It can be seen from Table 6 that the thermal conductivity values for pristine VIPs and aged VIPs, accounting for thermal bridges, and $\lambda_{90/90}$ ranges immensely from 0.00417 W/(mK) to 0.00728 W/(mK). As can be expected, the mean center-of-panel thermal conductivity values were the lowest, and the thermal conductivity values increased as thermal bridge was accounted for. The values further increased for aged VIPs. This is in agreement with conclusions in previous studies stating that the effects of thermal bridge and aging on the resultant thermal conductivity of a panel are somewhat significant [9,16]. While thermal conductivity based on 90% percentile values with 90% reliability ($\lambda_{90/90}$) introduces a factor of reliability or tolerance, this also increases the VIP thermal conductivity.

3.2. Building Energy Consumption Evaluations

To understand the impact of applying one thermal conductivity index over the other for full-scale building simulations, space heating and cooling demands for the reference building with installed VIPs (Section 2.3) were examined, based on the climatic conditions of Seongnam City, Republic of Korea. Seongnam City has a humid continental climate, which is characterized by large seasonal temperature differences, with warm to hot and humid summers and cold (sometimes severely cold) dry winters, typically classified as *Dwa* under Köppen climate classification [33]. The highest and lowest daytime mean ambient dry bulb temperatures in a year fluctuate from 34.0 °C to −13.4 °C. Daily humidity (RH) in the area ranged from 17% to 99%, with wind speeds as high as 10.8 m/s. During a representative hot summer day (i.e., 16 September), the horizontal solar radiation reached a peak of 840 W/m^2, corresponding to a peak outdoor ambient temperature of about 26.1 °C, just after midday. On the other hand, on a representative cold winter day (i.e., 8 February), horizontal solar radiation reached a peak of around 550 W/m^2, characterized by outdoor daytime temperatures between −3 °C to 6 °C. The ambient conditions for the representative summer and winter days are plotted in Figure 5.

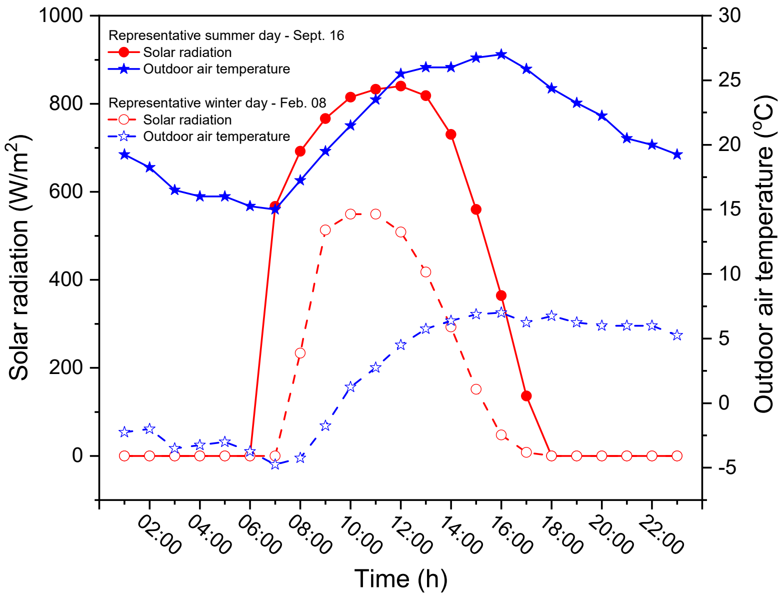

Figure 5. Fluctuation of solar radiation and ambient air temperature profiles for typical winter (8 February) and summer (16 September) days.

The space heating and cooling energy demands for the various thermal conductivity indexes are plotted in Figures 6 and 7, respectively.

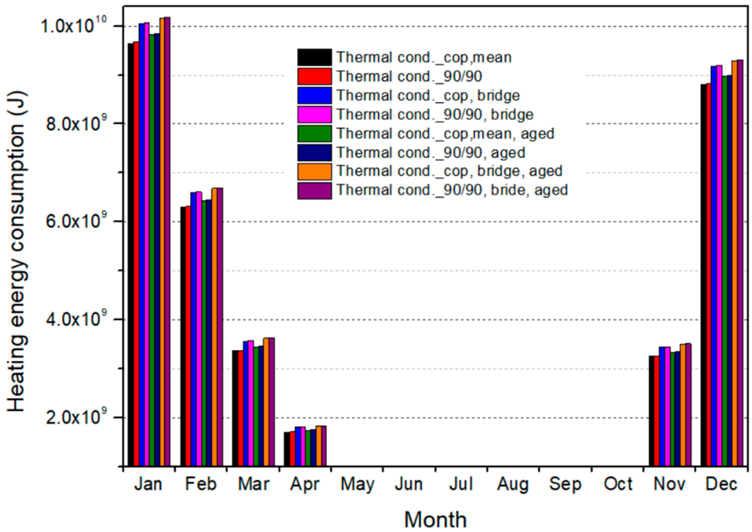

Figure 6. Heating energy demand.

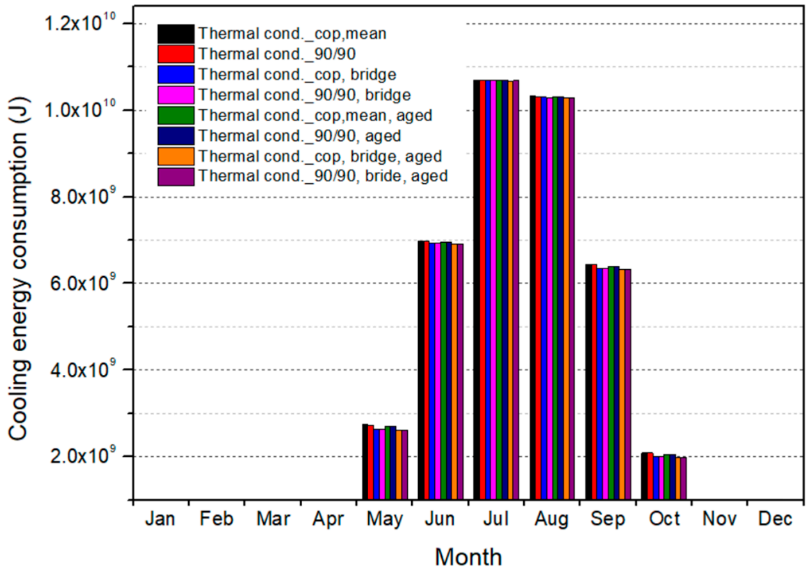

Figure 7. Cooling energy demand.

Generally, the impact of the thermal conductivity indexes was more noticeable during the heating season. Howbeit, there were some fluctuations for the cooling season as well. In Figure 6, the energy required for heating increased as factors such as thermal bridge and aging were computed. This is because accounting for such factors increased the thermal conductivity of VIPs (already reported in Table 6), which resulted in an undesirable increase in the *U*-value of the building fabric. For instance, the *U*-value of the building wall was 0.12 W/m^{2}K based on VIPs' center-of-panel thermal conductivity and increased to about 0.16 W/m^{2}K when computed with the thermal conductivity values based on 90% percentile values with 90% reliability, including factors for aging and thermal bridge. This corresponds to about a 33% increase in the *U*-value. Table 7 summarizes the resultant *U*-values for the reference building wall based on the thermal conductivity indexes for VIPs. Again, from Figure 6, it can be clearly deduced that the biggest heating energy differences were observed between #1 (λ_{cop}) and #8 $(\lambda_{90/90,\ \mathrm{bridge,aged}})$ thermal conductivity indexes, corresponding to about 2.1 GJ. The difference in heating energy between #3 $(\lambda_{cop,\mathrm{bridge}})$ and #1 (λ_{cop}) thermal conductivity indexes was about 1.6 GJ, while the difference was around 0.54 GJ between #3 $(\lambda_{cop,\mathrm{bridge}})$ and #8 $(\lambda_{90/90,\mathrm{bridge,aged}})$. Similarly, the difference in heating energy between #7 $(\lambda_{cop,\mathrm{bridge,aged}})$ and #3 $(\lambda_{cop,\mathrm{bridge}})$ thermal conductivity indexes was about 0.46 GJ, while the difference was around 0.08 GJ between #7 $(\lambda_{cop,\mathrm{bridge,aged}})$ and #8 $(\lambda_{90/90,\mathrm{bridge,aged}})$. Bearing in mind that #3 $(\lambda_{cop,\mathrm{bridge}})$ is most quoted in the literature, the results show that #7 $(\lambda_{cop,\mathrm{bridge,aged}})$ is sufficiently more reliable for energy modeling computations, especially when one is limited by the number of samples.

Table 7. Computed *U*-values for reference building walls based on the thermal conductivity indexes for VIPs.

Case #	Thermal Conductivity Indexes	*U*-Value of Wall
1	Mean center-of-panel thermal conductivity (λ_{cop})—0.00417 W/(mK)	0.120 W/(m^{2}K)
2	Thermal conductivity based on 90% percentile values with 90% reliability $(\lambda_{90/90})$—0.00427 W/(mK)	0.122 W/(m^{2}K)
3	Mean center-of-panel thermal conductivity, plus thermal bridge $(\lambda_{cop,\mathrm{bridge}})$—0.00630 W/(mK)	0.149 W/(m^{2}K)
4	Thermal conductivity based on 90% percentile values with 90% reliability, plus thermal bridge $(\lambda_{90/90,\mathrm{bridge}})$—0.00641 W/(mK)	0.150 W/(m^{2}K)

Table 7. *Cont.*

Case #	Thermal Conductivity Indexes	*U*-Value of Wall
5	Mean center-of-panel thermal conductivity, plus aging ($\lambda_{cop,\text{aged}}$)—0.00499 W/(mK)	0.132 W/(m^{2}K)
6	Thermal conductivity based on 90% percentile values with 90% reliability, plus aging ($\lambda_{90/90,\text{aged}}$)—0.00515 W/(mK)	0.135 W/(m^{2}K)
7	Mean center-of-panel thermal conductivity, plus aging and thermal bridge effects ($\lambda_{cop,\text{bridge,aged}}$)—0.00713 W/(mK)	0.158 W/(m^{2}K)
8	Thermal conductivity based on 90% percentile values with 90% reliability, plus thermal bridge, and aging effects ($\lambda_{90/90,\text{bridge,aged}}$)—0.00728 W/(mK)	0.159 W/(m^{2}K)

4. Limitations, Reflections, and Future Perspectives

4.1. Motivation and Challenges

From the initial United Nations Framework Convention on Climate Change (UNFCCC) Conference of the Parties (COP) 1, hosted in Berlin, Germany, in 1995, to the recent UNFCCC COP 27, held in Sharm el-Sheik, Egypt, in 2022, there has been greater awareness, resolutions, and policies enacted towards sustainable buildings, environments, and communities globally. Faced with the current changing climate and strict building codes around the globe, due to their high thermal performance, vacuum insulation panels (VIPs) have been installed in buildings for close to three decades now. One peculiar characteristic of VIPs is that, unlike other conventional building insulation materials, they are not homogenous. Rather, it is composed of a core material encapsulated in a gas-tight envelope, which introduces thermal bridges and other factors when analyzing VIPs' resultant thermal conductivity. Because of this same reason, different approaches are used to model VIPs in energy simulations. The commonest approach involves factoring the thermal bridge effect together with the thermal conductivity and inputting it as the effective thermal conductivity of VIPs. Nonetheless, other thermal conductivity indexes that may be more accurate and reliable for energy simulations exist. This was the core motivation of this study.

4.2. Future Research Opportunities

Some notable thermal conductivity indexes of VIPs, such as the center-of-panel thermal conductivity, center-of-panel thermal conductivity plus thermal bridges, and, in some cases, the aging effect on the center-of-panel thermal conductivity, have been widely reported in the open literature, but published works on other indexes, particularly thermal conductivity, based on 90% percentile values with 90% reliability ($\lambda_{90/90}$), are very rare. The authors could only access one study on the subject. Nonetheless, evaluating the energy implications of the thermal conductivity index was beyond the scope of the study, so it was not investigated. To that effect and more, this study was designed. Nonetheless, this study is also restricted by the scope considered. The authors focused on a wooden wall structure installed with VIPs for a residential building; therefore, the results can be replicated for such a system. Clearly, there is a need for similar assessments on other types of wall systems and under different environmental conditions as well.

5. Conclusions and Outlook

In this study, experimental and numerical procedures were employed to investigate the thermal characteristics of vacuum insulation panels (VIPs). In particular, by utilizing guidelines under development (ISO DIS 16478), various thermal conductivity scenarios for VIPs were determined, and their corresponding impact on building energy consumption was evaluated based on a reference building with VIPs installed on the external wall. Overall, eight thermal conductivity indexes were investigated. In the context of this study, the term thermal conductivity index is primarily used to refer to possible thermal conductivity values for VIPs, considering or not considering factors such as thermal bridges, aging, and the 90% percentile with a reliability of 90%.

Results show that the specific thermal conductivity values of VIPs have a pronounced effect on the overall *U*-value of the building wall. From an energy modeling perspective, the biggest difference in annual heating energy load (2.1 GJ) was observed between the thermal conductivity value measured for a pristine VIP at the center of the panel (λ_{cop}) and the thermal conductivity value based on 90% percentile values with 90% reliability, including factors for aging and thermal bridge ($\lambda_{90/90,\ \mathrm{bridge,aged}}$). The $\lambda_{90/90,}$ bridge, aged value introduces a factor of reliability or tolerance, which considers production deviation as well. Consequently, computations based on the $\lambda_{90/90,}$ bridge, aged value yielded the highest total energy loads. Nonetheless, given that its resultant energy load calculations were sufficiently close to that for $\lambda_{90/90,\mathrm{bridge,aged}}$ value, it was found that the mean center-of-panel thermal conductivity value, accounting for thermal bridge and aging effects ($\lambda_{cop,\mathrm{bridge,aged}}$), is more reliable for energy modeling than the frequently used mean center-of-panel thermal conductivity, considering thermal bridges only ($\lambda_{cop,\mathrm{bridge}}$).

To concretely define the scope and applicability of this study, input parameters have been reported in detail. Limitations of the modeling methods used and opportunities for possible future research have been discussed as well. For instance, future works on the subject could consider other types of wall systems other than the wooden wall systems used in this study. Overall, VIP technology is a progressive thermal insulation solution for building applications. To properly model a building, various building components and systems should be accurately represented. Although sophisticated building performance software exists, user inputs still have a tremendous effect. Thus, it is imperative to verify the thermal conductivity value for VIPs since its effect on the overall building envelope *U*-value and energy loads cannot be marginalized. This study will be interesting to researchers and scientists in the built environment discipline, engineers, and general stakeholders in the building industry.

Author Contributions: Conceptualization, F.E.B., J.-T.K. and J.-H.K.; methodology, F.E.B. and J.-T.K.; software, F.E.B. and S.-M.K.; validation, F.E.B., J.-H.K. and J.-G.A.; formal analysis, F.E.B., J.-G.A. and S.-M.K.; investigation, F.E.B. and S.-M.K.; data curation, F.E.B.; writing—original draft preparation, F.E.B.; writing—review and editing, F.E.B., J.-H.K. and J.-T.K.; visualization, F.E.B. and J.-G.A.; supervision, J.-T.K.; project administration, J.-H.K.; funding acquisition, J.-T.K. All authors have read and agreed to the published version of the manuscript.

Funding: This work was funded by the Korea Institute of Energy Technology Evaluation and Planning (KETEP) through the Ministry of Trade, Industry, and Energy (MOTIE) of the Republic of Korea (No. 20202020800360) and also supported by a research grant from Kongju National University in 2020.

Data Availability Statement: The data presented in this study are available on request by contacting the corresponding author.

Conflicts of Interest: The authors declare no conflict of interest.

References

1. Baetens, R.; Jelle, B.P.; Thue, J.V.; Tenpierik, M.J.; Grynning, S.; Uvsløkk, S.; Gustavsen, A. Vacuum insulation panels for building applications: A review and beyond. *Energy Build.* **2010**, *42*, 147–172. [CrossRef]
2. Boafo, F.E.; Chen, Z.; Li, C.; Li, B.; Xu, T. Structure of vacuum insulation panel in building system. *Energy Build.* **2014**, *85*, 644–653. [CrossRef]
3. Abu-Jdayil, B.; Mourad, A.-H.; Hittini, W.; Hassan, M.; Hameedi, S. Traditional, state-of-the-art and renewable thermal building insulation materials: An overview. *Constr. Build. Mater.* **2019**, *214*, 709–735. [CrossRef]
4. Brunner, S.; Wakili, K.G.; Stahl, T.; Binder, B. Vacuum insulation panels for building applications—Continuous challenges and developments. *Energy Build.* **2014**, *85*, 592–596. [CrossRef]
5. Chen, Z.; Chen, Z.; Yang, Z.; Hu, J.; Yang, Y.; Chang, L.; Lee, L.J.; Xu, T. Preparation and characterization of vacuum insulation panels with super-stratified glass fiber core material. *Energy* **2015**, *93*, 945–954. [CrossRef]
6. Quenard, D.; Sallée, H.; d'Heres, C.G.-S.M. From VIP's to building facades: Three levels of thermal bridges. In Proceedings of the 7th International Vacuum Insulation Symposium, Duebendorf, Switzerland, 28–29 September 2005.
7. Lorenzati, A.; Fantucci, S.; Capozzoli, A.; Perino, M. The effect of different materials joint in Vacuum Insulation Panels. *Energy Procedia* **2014**, *62*, 374–381. [CrossRef]

8. Boafo, F.E.; Kim, J.-H.; Ahn, J.-G.; Kim, S.-M.; Kim, J.-T. Slim curtain wall spandrel integrated with vacuum insulation panel: A state-of-the-art review and future opportunities. *J. Build. Eng.* **2021**, *42*, 102445. [CrossRef]
9. Wakili, K.G.; Bundi, R.; Binder, B. Effective thermal conductivity of vacuum insulation panels. *Build. Res. Inf.* **2004**, *32*, 293–299. [CrossRef]
10. Simmler, H.; Brunner, S. Vacuum insulation panels for building application: Basic properties, aging mechanisms and service life. *Energy Build.* **2005**, *37*, 1122–1131. [CrossRef]
11. Simmler, H.; Brunner, S.; Heinemann, U.; Schwab, H.; Kumaran, K.; Mukhopadhyaya, P.; Quénard, D.; Sallée, H.; Noller, K.; Kücükpinar-Niarchos, E.; et al. IEA/ECBCS Annex 39 (Subtask A). In *Vacuum Insulation Panels: Study on VIP-Components and Panels for Service Life Prediction of VIP in Building Applications*; IEA/ECBS Annex 39: Paris, France, 2005.
12. Brunner, S.; Wakili, K.G. Hints for an additional aging factor regarding the thermal performance of vacuum insulation panels with pyrogenic silica core. *Vacuum* **2014**, *100*, 4–6. [CrossRef]
13. *ISO/DIS 16478*; Thermal Insulation Products for Buildiings—Vacuum Insulation Panels (VIP)—Products Specification. ISO: Geneva, Switzerland, 2018.
14. Brunner, S.; Stahl, T.; Wakili, K.G. Double layered vacuum insulation panels. In Proceedings of the 3rd Building Enclosure Science and Technology (BEST3) Conference, Atlanta, GA, USA, 2–4 April 2012.
15. Lorenzati, A.; Fantucci, S.; Capozzoli, A.; Perino, M. Experimental and numerical investigation of thermal bridging effects of jointed Vacuum Insula-tion Panels. *Energy Build.* **2016**, *111*, 164–175. [CrossRef]
16. Boafo, F.E.; Kim, J.-H.; Kim, J.-T. Numerical study of slim curtain wall spandrel with integrated vacuum insulation panel: Concept, performance evaluation and challenges. *Energy Build.* **2019**, *183*, 139–150. [CrossRef]
17. Boafo, F.E.; Kim, J.-H.; Ahn, J.-G.; Kim, S.-M.; Kim, J.-T.; Zhang, L. Study on thermal characteristics and electrical performance of a hybrid building integrated photovoltaic (BIPV) system combined with vacuum insulation panel (VIP). *Energy Build.* **2022**, *277*, 112574. [CrossRef]
18. Batard, A.; Duforestel, T.; Flandin, L.; Yrieix, B. Modelling of long-term hygro-thermal behaviour of vacuum insulation panels. *Energy Build.* **2018**, *173*, 252–267. [CrossRef]
19. Park, S.; Choi, B.-H.; Lim, J.-H.; Song, S.-Y. Evaluation of Mechanically and Adhesively Fixed External Insulation Systems Using Vacuum Insulation Panels for High-Rise Apartment Buildings. *Energies* **2014**, *7*, 5764–5786. [CrossRef]
20. Kim, S.-M.; Kim, J.-T. Effect of thermal bridge on the insulation performance of VIP applied walls. In Proceedings of the 6th ZEMCH International Conference, Melbourne, Australia, 28 January–5 February 2018.
21. *BS EN 13162*; Thermal Insulation Products for Buildings—Factory Made Mineral Wool (MW) Products—Specification. BSI: London, UK, 2013.
22. *BS EN 13163*; Thermal Insulation Products for Buildings—Factory Made Expanded Polystyrene (EPS) Products—Specification. BSI: London, UK, 2012.
23. *BS EN 13164*; Thermal Insulation Products for Buildings—Factory Made Extruded Polystyrene Foam (XPS) Products—Specification. BSI: London, UK, 2012.
24. *BS EN 13165*; Thermal Insulation Products for Buildings—Factory Made Rigid Polyurethane Foam (PU)—Specification. BSI: London, UK, 2012.
25. *BS EN 13166*; Thermal Insulation Products for Buildings—Factory Made Phenolic Foam (PF)—Specification. BSI: London, UK, 2012.
26. *BS EN 13167*; Thermal Insulation Products for Buildings—Factory Made Cellular Glass (CG) Products—Specification. BSI: London, UK, 2012.
27. Wu, W.P.; Chen, Z.F.; Zhou, J.M.; Cheng, X.Y. Thermal Properties of Vacuum Insulation Panels with Glass Fiber. *Adv. Mater. Res.* **2012**, *446*, 3753–3756. [CrossRef]
28. NETZSCH. Heat Flow Meter 436 Series. Available online: https://analyzing-testing.netzsch.com/_Resources/Persistent/7/4/b/2/74b2ff23165fad3f0d0659d00b2dc095ae3eb5cb/2008_Brochure_HFM_436_E_0608.pdf (accessed on 1 August 2023).
29. Adl-Zarrabi, B.; Quénard, D.; Yrieix, B.; Johansson, P.; Heinemann, U.; Sprengard, C.; Mukhopadhyaya, P.; Brunner, S.; Galliano, R.; Lorenzati, A.; et al. IEA EBC Annex 65 Long Term Performance of Super-Insulating Materials in Building Components and Systems, Subtask III—Practical Applications Retrofitting at the Building Scale, Final Report. 2020. Available online: https://www.iea-ebc.org/projects/project?AnnexID=65 (accessed on 30 January 2023).
30. *ISO 10292*; Glass in Building—Calculation of Steady State U Values (Thermal Transmittance) of Multiple Glazing. ISO: Geneva, Switzerland, 1994.
31. DesignBuilder Software. Available online: https://designbuilder.co.uk/certification (accessed on 6 July 2023).
32. US Department of Energy, EnergyPlus Input Output Reference—The Encyclopedic Reference to EnergyPlus Input and Output, EnergyPlus Documentation. 2013, p. 1836. Available online: https://bigladdersoftware.com/epx/docs/9-4/input-output-reference/ (accessed on 2 August 2023).
33. Peel, M.C.; Finlayson, B.L.; McMahon, T.A. Updated world map of the Köppen-Geiger climate classification. *Hydrol. Earth Syst. Sci.* **2007**, *11*, 1633–1644. [CrossRef]